AGU PUBLICATIONS

JGR

Journal of Geophysical Research: Atmospheres

RESEARCH ARTICLE
10.1002/2014JD022627

**Key Points:**
- NEI08 overestimates the toluene flux by >3× mostly due to biased non-road source
- NEI08 underestimates on-road benzene and $C_8$ aromatic flux during the warm season
- Long-range transport exerts an important impact on ambient benzene over the US

**Supporting Information:**
- Readme
- Figure S1
- Figure S2
- Figure S3
- Figure S4
- Figure S5
- Tables S1–S3

**Correspondence to:**
D. B. Millet,
dbm@umn.edu

**Citation:**
Hu, L., et al. (2015), Emissions of $C_6$–$C_8$ aromatic compounds in the United States: Constraints from tall tower and aircraft measurements, *J. Geophys. Res. Atmos.*, *120*, doi:10.1002/2014JD022627.

Received 25 SEP 2014
Accepted 12 DEC 2014
Accepted article online 17 DEC 2014

# Emissions of $C_6$–$C_8$ aromatic compounds in the United States: Constraints from tall tower and aircraft measurements

**Lu Hu[1,2], Dylan B. Millet[1], Munkhbayar Baasandorj[1], Timothy J. Griffis[1], Katherine R. Travis[2], Christopher W. Tessum[3], Julian D. Marshall[3], Wesley F. Reinhart[1], Tomas Mikoviny[4,5], Markus Müller[6], Armin Wisthaler[4,6], Martin Graus[7,8,9], Carsten Warneke[7,8], and Joost de Gouw[7,8]**

[1]Department of Soil, Water, and Climate, University of Minnesota, St. Paul, Minnesota, USA, [2]School of Engineering and Applied Sciences, Harvard University, Cambridge, Massachusetts, USA, [3]Department of Civil, Environmental, and Geo-Engineering, University of Minnesota, Minneapolis, Minnesota, USA, [4]Department of Chemistry, University of Oslo, Oslo, Norway, [5]Oak Ridge Associated Universities, Oak Ridge, Tennessee, USA, [6]Institute of Ion Physics and Applied Physics, University of Innsbruck, Innsbruck, Austria, [7]Cooperative Institute for Research in Environmental Sciences, University of Colorado, Boulder, Colorado, USA, [8]Chemical Sciences Division, Earth System Research Laboratory, NOAA, Boulder, Colorado, USA, [9]Now at Institute of Meteorology and Geophysics, University of Innsbruck, Innsbruck, Austria

**Abstract** We present two full years of continuous $C_6$–$C_8$ aromatic compound measurements by PTR-MS at the KCMP tall tower (Minnesota, US) and employ GEOS-Chem nested grid simulations in a Bayesian inversion to interpret the data in terms of new constraints on US aromatic emissions. Based on the tall tower data, we find that the RETRO inventory (year-2000) overestimates US $C_6$–$C_8$ aromatic emissions by factors of 2.0–4.5 during 2010–2011, likely due in part to post-2000 reductions. Likewise, our implementation of the US EPA's NEI08 overestimates the toluene flux by threefold, reflecting an inventory bias in non-road emissions plus uncertainties associated with species lumping. Our annual top-down emission estimates for benzene and $C_8$ aromatics agree with the NEI08 bottom-up values, as does the inferred contribution from non-road sources. However, the NEI08 appears to underestimate on-road emissions of these compounds by twofold during the warm season. The implied aromatic sources upwind of North America are more than double the prior estimates, suggesting a substantial underestimate of East Asian emissions, or large increases there since 2000. Long-range transport exerts an important influence on ambient benzene over the US: on average 43% of its wintertime abundance in the US Upper Midwest is due to sources outside North America. Independent aircraft measurements show that the inventory biases found here for $C_6$–$C_8$ aromatics also apply to other parts of the US, with notable exceptions for toluene in California and Houston, Texas. Our best estimates of year-2011 contiguous US emissions are 206 (benzene), 408 (toluene), and 822 ($C_8$ aromatics) GgC.

## 1. Introduction

Aromatic volatile organic compounds (VOCs) such as benzene ($C_6H_6$), toluene ($C_7H_8$), xylenes ($C_8H_{10}$; including *o*-, *m*-, *p*-isomers), and ethylbenzene (also $C_8H_{10}$) are ubiquitous in the atmosphere and are important anthropogenic precursors of secondary organic aerosol [*Johnson et al.*, 2005; *Martín-Reviejo and Wirtz*, 2005; *Ng et al.*, 2007; *Henze et al.*, 2008], peroxy acetyl nitrate (PAN) [*Liu et al.*, 2010], and, to a lesser degree, ground-level ozone [*Ahmadov et al.*, 2014; *Jaars et al.*, 2014; *Xue et al.*, 2014]. These aromatic VOCs (so-called BTEX compounds) are categorized as hazardous air pollutants (HAPs) under the US Clean Air Act Amendments of 1990 (http://www.epa.gov/ttnatw01/orig189.html), as they are known or suspected to cause serious health effects. For instance, benzene is classified as a Group 1 carcinogen by the International Agency for Research on Cancer [*Baan et al.*, 2009]. Despite their importance, emissions of aromatic compounds remain poorly quantified. In this work, we present 2 years of continuous aromatic VOC measurements from a tall tower in the Upper Midwest of the United States. We apply a nested chemical transport model (GEOS-Chem CTM) to interpret these data, along with an ensemble of recent aircraft observations, in terms of the constraints they imply for US sources of $C_6$–$C_8$ aromatic compounds.

Atmospheric $C_6$–$C_8$ aromatic compounds are emitted from a range of urban and industrial sources as well as from open and domestic biomass burning [*Andreae and Merlet*, 2001; *Akagi et al.*, 2011]. The former include vehicular emissions (on-road and off-road) associated with the incomplete combustion and evaporation of fuel,

stationary sources such as industrial surface coating and solvent use, gas stations, refineries, power plants, and waste treatment facilities [*Singh et al.*, 1985; *Kaiser et al.*, 1992; *Harley et al.*, 2006; *Karl et al.*, 2009; *Jaars et al.*, 2014]. Throughout this study, we use the term "non-road" emissions to refer to the sum of stationary, area, and off-road sources, i.e., all anthropogenic sources except those from on-road vehicle transportation (and fires). Certain crops and coniferous trees (specifically alfalfa and pine) have also been found to emit toluene [*White et al.*, 2009], but the overall impact of biogenic toluene emissions is probably minor compared to the anthropogenic and pyrogenic sources. The atmospheric removal of $C_6$–$C_8$ aromatic compounds is almost exclusively through oxidation by OH, resulting in atmospheric lifetimes of about 10 days for benzene, 2 days for toluene, and 1 day or less for ethylbenzene and xylenes (at OH = $10^6$ molecules $cm^{-3}$) [*Atkinson et al.*, 2006].

Recent top-down studies imply the presence of large uncertainties in current bottom-up emission estimates for $C_6$–$C_8$ aromatic compounds. For instance, *Fortin et al.* [2005] applied ambient benzene : acetylene ratios from a variety of field experiments to infer a 56% drop in US benzene emissions between 1994 and 2003. This finding contradicted available bottom-up information from the EPA's National Emission Inventory (NEI99), which predicted benzene : acetylene emission ratios 3–4 times higher than could be reconciled with atmospheric data [*Parrish*, 2006]. Evidence from tall tower, mobile laboratory [*Pétron et al.*, 2012], and aircraft-based observations [*Pétron et al.*, 2014] suggests that benzene sources from oil and gas operations in northeastern Colorado are underestimated in the state emission inventory [*Bar-Ilan et al.*, 2008; *CDPHE*, 2008] by a factor of 6, though with a high degree of uncertainty [*Levi,* 2012, 2013]. On the other hand, *Warneke et al.* [2007] found that their model simulation for 2004 based on the EPA's NEI99 inventory overpredicted toluene mixing ratios in the New England area by a factor of 3, suggesting a large emission overestimate for that compound. A recent top-down estimate for East Asian aromatic emissions (based on satellite measurements of glyoxal) is about 6 times larger than predicted by current bottom-up inventories [*Liu et al.*, 2012]: if true, this would imply that long-range transport is a more substantial source of aromatic VOCs over the US than is presently thought, at least in the case of benzene with its longer atmospheric lifetime.

In this study, we aim to develop an improved understanding of aromatic VOC emissions in the United States. We combine 2 years of continuous in situ observations from a tall tower in the US Upper Midwest (KCMP tall tower) with a $0.5° \times 0.667°$ nested version of the GEOS-Chem CTM in an inverse framework to derive optimized emission estimates for $C_6$ (benzene), $C_7$ (toluene), and $C_8$ (ethylbenzene + *m*-, *o*-, and *p*-xylene) aromatic compounds. We then apply independent measurements from six recent aircraft campaigns across the contiguous US to test the national representativeness of our findings.

## 2. Methods

### 2.1. KCMP Tall Tower Measurements

The KCMP tall tower (44.6886°N, 93.0728°W; 244 m height; Figure 1) is in a rural location, 29 km south of downtown St. Paul, MN, US. Measurements at the tower were initialized in April 2007, and subsequent studies have employed data from this site to advance our understanding of land-atmosphere interactions and surface fluxes of greenhouse gases and reactive trace species such as carbon dioxide [*Griffis et al.*, 2010], nitrous oxide [*Griffis et al.*, 2013; *Zhang et al.*, 2014a], methane [*Zhang et al.*, 2014b, 2014c], methanol [*Hu et al.*, 2011; *Wells et al.*, 2012], acetone [*Hu et al.*, 2013], isoprene and its oxidation products (L. Hu et al., Isoprene emissions and impacts over an ecological transition region in the US Upper Midwest inferred from tall tower measurements, submitted to *Journal of Geophysical Research*, 2015), and carbon monoxide [*Kim et al.*, 2013].

We used a high-sensitivity proton transfer reaction quadrupole mass spectrometer (PTR-MS, Ionicon Analytik, Austria) to measure a suite of VOCs including $C_6$–$C_8$ aromatic compounds every ~3 min between July 2009 and August 2012. During the campaign, the PTR-MS was operated at ~130–140 Td with a drift tube pressure of 2.1–2.3 mbar, drift tube voltage of 600 V, reaction chamber temperature of 60 °C, and extraction voltages at 50 V. Measurements were made at a sampling height of 185 m above ground level, thus providing a temporally resolved dataset with a regional-scale footprint [e.g., see *Kim et al.*, 2013, Figure 2]. The PTR-MS was calibrated automatically using a 6-point standard curve every 23 h or every 47 h (before or after August 2010, respectively), generated by dynamic dilution of multicomponent standards into zero air. The latter was created by passing ambient air through a heated platinum bead catalyst (450 °C; Shimadzu Corp., Japan). The VOC standard cylinders were originally filled in December 2008 (Apel-Riemer, Inc., US) and were recalibrated in November 2013 (31 ppbv for benzene, 35 ppbv for toluene, and 44 ppbv for *p*-xylene) using a custom-built permeation system employing a

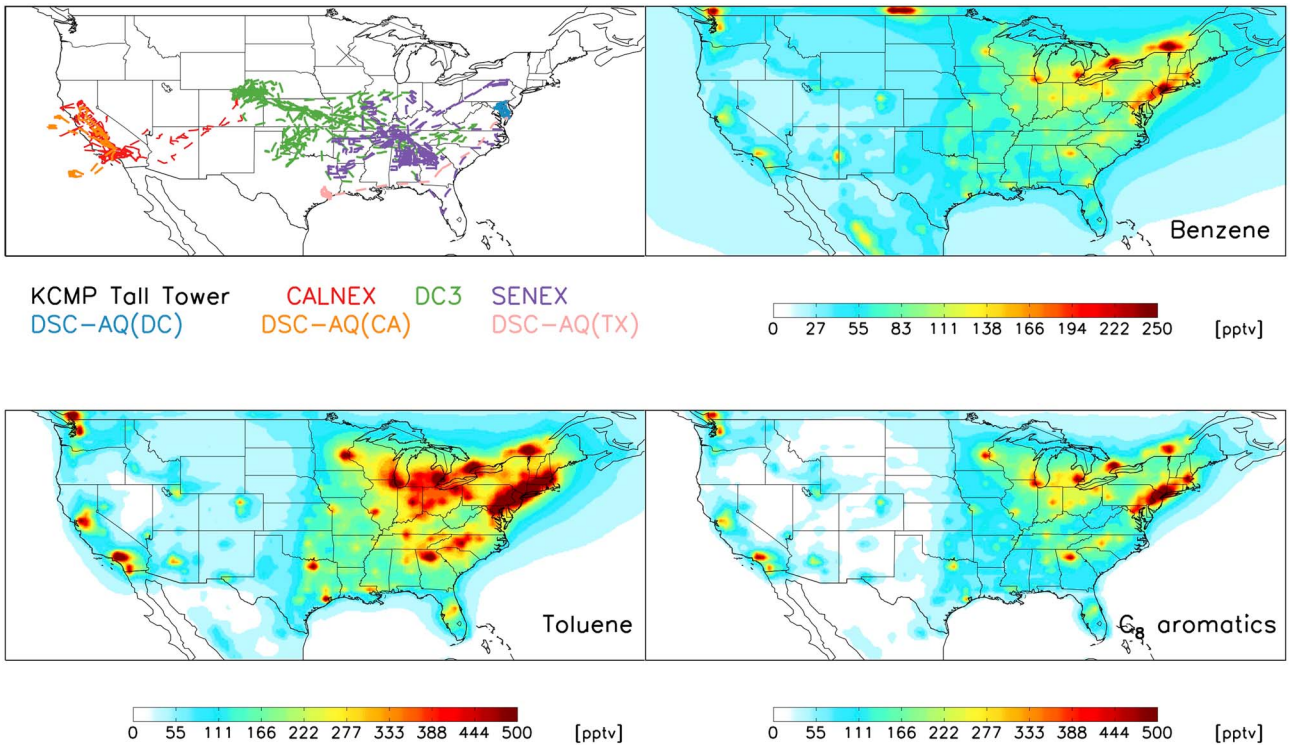


**Figure 1.** Simulated surface mixing ratios ($P > 900$ hPa; annual mean) of $C_6$–$C_8$ aromatic compounds over the contingous US for the year 2011, according to the base-case GEOS-Chem simulation using the NEI08 emission inventory. Also shown (top left panel) is the location of the KCMP tall tower, along with flight tracks for the six aircraft campaigns used in this study. DSC-AQ (CA): DISCOVER-AQ California; DSC-AQ (DC): DISCOVER-AQ Baltimore-Washington, DC; DSC-AQ (TX): DISCOVER-AQ Texas.

heated catalyst and a $CO_2$ sensor (LI-840A, Li-COR Environmental, US) to quantify the VOC concentration in the calibration stream [*Veres et al.*, 2010; *Baasandorj et al.*, 2014]. The PTR-MS measures all $C_8$ aromatic compounds at *m/z* 107; here we use the approach of *de Gouw et al.* [2003] to calculate a weighted calibration factor for the sum of $C_8$ aromatics based on the measured *p*-xylene sensitivity and its typical abundance relative to its isomers.

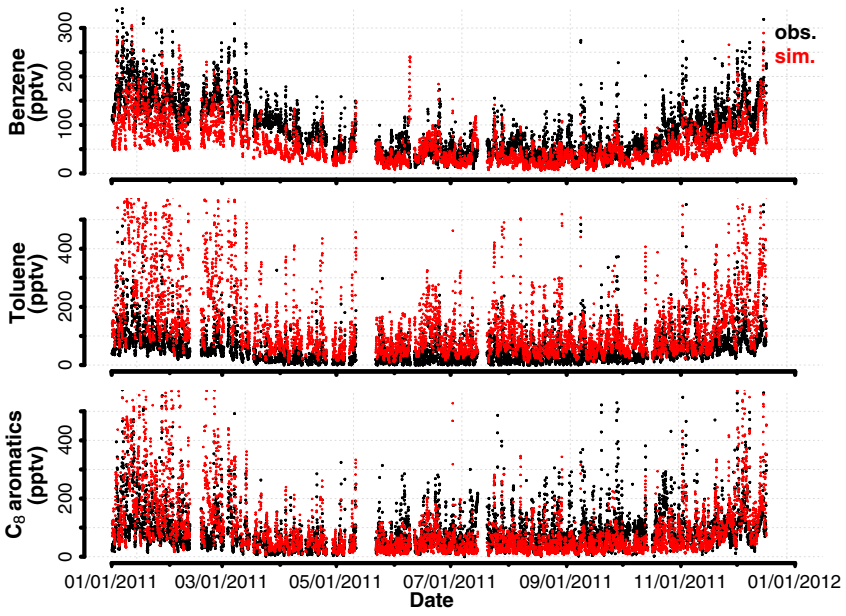


**Figure 2.** Annual cycle in benzene, toluene, and $C_8$ aromatics observed at the KCMP tall tower during 2011 (black). The GEOS-Chem a priori simulation based on the EPA's NEI08 inventory is shown in red. All data points are 1 h means.

**Table 1.** Datasets Used in This Work

| Campaign | Timeframe | Location | Instrument | PI (Reference) |
|---|---|---|---|---|
| KCMP tall tower | 2010–2011 | MN, US | PTR-MS | Millet (http://www.atmoschem.umn.edu/data.htm) |
| DC3 | May/June 2012 | Central US | PTR-MS | Wisthaler (http://www2.acd.ucar.edu/dc3) |
| DISCOVER-AQ California | January/February 2013 | San Joaquin Valley, CA, US | PTR-ToF-MS | Wisthaler (http://discover-aq.larc.nasa.gov/) |
| DISCOVER-AQ Baltimore-Washington, DC | June/July 2011 | Baltimore, MD, US / Washington, DC, US | PTR-MS | Wisthaler (http://discover-aq.larc.nasa.gov/) |
| CALNEX | May/June 2010 | CA, US | PTR-MS | de Gouw (http://www.esrl.noaa.gov/csd/projects/calnex) |
| SENEX | June/July 2013 | Southeastern US | PTR-MS | de Gouw (http://www.esrl.noaa.gov/csd/projects/senex/) |
| DISCOVER-AQ Texas | September 2013 | Houston, TX, US | PTR-ToF-MS | Wisthaler (http://discover-aq.larc.nasa.gov/) |

In this work, we use hourly averaged molar mixing ratios of benzene ($C_6$; measured as protonated *m/z* 79 by PTR-MS), toluene ($C_7$; protonated m/z 93), and $C_8$ aromatic compounds (protonated *m/z* 107; ethylbenzene + *m*-, *o*-, and *p*-xylene) measured at the KCMP tall tower during 2010 and 2011. We tested the acetic acid interference at *m/z* 79 and found that for the instrumental conditions employed here, PTR-MS sensitivity to the acetic acid-water cluster is much smaller than the sensitivity to benzene ($<$ 0.1 ncps/ppbv versus ~10 ncps/ppbv under the above conditions) [*Baasandorj et al.*, 2014]. Other potential interferences for measurements of $C_6$–$C_8$ aromatics by quadrupole PTR-MS have been found to be minor [*Warneke et al.*, 2001; *de Gouw et al.*, 2003; *de Gouw and Warneke*, 2007]. Detection limits (defined as 3× the precision) were approximately 17 pptv, 20 pptv, and 30 pptv for benzene, toluene, and $C_8$ aromatics based on a 10 s dwell time. The total measurement uncertainty is calculated hourly based on the sum of the detection limit and a relative error propagated from the main sources of instrumental uncertainty (mass flow measurement, calibration factors and fit, mixing ratio standard errors for each averaging interval, etc.). The total hourly uncertainty calculated in this way averages $\leq$10% for benzene and $C_8$ aromatics, and $<$20% for toluene. A more detailed description of the measurement methods and the field site is provided in earlier papers [*Hu et al.*, 2011, 2013]. All data presented here, along with concurrent measurements of other VOCs and CO at the KCMP tall tower, are available for download at http://www.atmoschem.umn.edu/data.htm.

### 2.2. Aircraft Observations

We use airborne observations from six recent aircraft studies over the US (Table 1 and Figure 1) to test the broader representativeness of our findings from the tall tower measurements. These include CALNEX (California; May/June 2010), DISCOVER-AQ Baltimore-Washington DC (July 2011), DC3 (Central US; May/June 2012), DISCOVER-AQ California (January/February 2013), SENEX (Southeastern US; June/July 2013), and DISCOVER-AQ Texas (September 2013). A proton transfer reaction time-of-flight mass spectrometer (PTR-ToF-MS) was used to measure mixing ratios of $C_6$–$C_8$ aromatics (and an array of other compounds) during the DISCOVER-AQ California and Texas campaigns [*Müller et al.*, 2014], while quadrupole PTR-MS was used for the other studies (Table 1). As shown in Figure 1, the aircraft campaigns span a range of urban, rural, and remote areas across the Western, Central, Southern, and Eastern US. They thus provide a useful counterpoint to the tall tower measurements for assessing the extent that emission biases found for the US Upper Midwest appear to manifest in other areas of the contiguous US.

### 2.3. GEOS-Chem Forward Model

We use the GEOS-Chem CTM (version 9.1.3) to interpret the KCMP tall tower and aircraft observations in terms of their constraints on US $C_6$–$C_8$ aromatic emissions. GEOS-Chem is an Eulerian CTM [*Bey et al.*, 2001] driven by NASA Goddard Earth Observing System assimilated meteorological fields (GEOS-5.2.0). In this work, we use a nested-grid full-chemistry simulation over North America for 2010 and 2011. The nested domain covers 10°–70°N and 140°–40°W, with 0.5° × 0.667° horizontal resolution (latitude by longitude; approximately 56 km × 53 km at 45°N) and 47 vertical layers extending up to 0.01 hPa (14 layers are below

**Table 2.** Speciation of $C_6$–$C_8$ Aromatic Compounds for the PTR-MS Measurements and in the EPA NEI08 and RETRO Inventories as Used Here

| | | NEI08 CB05 | | RETRO | | |
|---|---|---|---|---|---|---|
| Species | PTR-MS | | US Emissions (2011, GgC) | | US Emissions (2000, GgC) | Global Emissions (2000, GgC) |
| Benzene | Benzene | Benzene | 187 | Benzene | 420 | 3212 |
| Toluene | Toluene | Toluene and other monoalkyl aromatics such as ethlybenzene | 961 | Toluene | 1448 | 5601 |
| $C_8$ aromatics | ethylbenzene + *m*-, *o*-, and *p*-xylene | Xylenes and other polyalkyl aromatics | 865 | Ethylbenzene + *m*-, *o*-, and *p*-xylene | 2009 | 7220 |

2 km altitude). Model transport is computed on a 10 min time step, while emissions and chemistry are computed on a 20 min time step. A 1 year spin-up for 2009 is used to minimize any effects from initial conditions. Lateral boundary conditions (for all species, at each vertical layer) for the nested grid simulations are based on 3-hourly output from global simulations carried out at $4° \times 5°$ resolution.

GEOS-Chem includes detailed $HO_x$–$NO_x$–VOC-ozone chemistry coupled to aerosols as originally described by *Bey et al.* [2001]. Details regarding more recent model developments and updates can be found at www.geos-chem.org. Here we describe aspects of the simulation most salient to the work presented in this paper.

The GEOS-Chem chemical mechanism, described by *Mao et al.* [2010], includes the most recent JPL/IUPAC recommendations, with isoprene oxidation following the scheme of *Paulot et al.* [2009a, 2009b]. Oxidation of benzene and toluene by OH is calculated using rate coefficients of $2.30 \times 10^{-12}$ exp[−190/*T*] $cm^3$ $molecule^{-1}$ $s^{-1}$ for benzene and $1.80 \times 10^{-12}$ exp[340/*T*] $cm^3$ $molecule^{-1}$ $s^{-1}$ for toluene [*Atkinson et al.*, 2006]. For $C_8$ aromatics, a weighted reaction rate coefficient of $1.5 \times 10^{-11}$ $cm^3$ $molecule^{-1}$ $s^{-1}$ is used based on the observed concentration ratios of *m*-xylene, *o*-xylene, *p*-xylene, and ethylbenzene from an ensemble of field campaigns [*Jacob et al.*, 2003; *Millet et al.*, 2004, 2005, 2006; *Singh et al.*, 2006; *Murphy et al.*, 2007; *Singh et al.*, 2009; *Toon et al.*, 2010]. To our knowledge, there are no published estimates of the deposition rates for $C_6$–$C_8$ aromatic compounds, and by default, these species do not undergo dry deposition in GEOS-Chem. For the simulations here, we implement dry deposition for $C_6$–$C_8$ aromatic compounds using a standard resistance-in-series model [*Wesely*, 1989] and Henry's law constants of 0.18, 0.16, and 0.15 M $atm^{-1}$ for benzene, toluene, and $C_8$ aromatic compounds, respectively [*Sander*, 1999]. Later (section 7), we conduct an uncertainty analysis to test the sensitivity of our results to model treatment of dry deposition.

Biomass burning emissions of $C_6$–$C_8$ aromatic and other chemical species are based on the monthly GFED3 inventory (Global Fire Emission Database version 3) [*van der Werf et al.*, 2010] and measured species: species open fire emission ratios [*Andreae and Merlet*, 2001]. Global anthropogenic emissions of CO, $NO_x$, and $SO_2$ in GEOS-Chem are based on the EDGAR monthly inventory (Emissions Database for Global Atmospheric Research) [*Olivier and Berdowski*, 2001]. For anthropogenic VOCs including $C_6$–$C_8$ aromatic compounds, we use here the RETRO (REanalysis of the TROpospheric chemical composition) [*Schultz et al.*, 2007] and the EPA NEI08 (National Emission Inventory for 2008; http://www.epa.gov/ttnchie1/net/2008report.pdf) emission inventories.

RETRO (version 2; available at ftp://ftp.retro.enes.org/) is a $0.5° \times 0.5°$ anthropogenic inventory, containing monthly global emissions for 24 distinct chemical species from 1960 to 2000 [*Schultz et al.*, 2007]. RETRO estimates emissions based on both economic (e.g., activity rates) and technological (e.g., emission factors for each activity) considerations, while also incorporating behavioral aspects (e.g., effects of investments in new or improved technologies) when estimating the time dependence of anthropogenic emissions, so that an emission factor is determined for each specific technology within every activity [*Schultz et al.*, 2007]. We implement the monthly RETRO emission inventory in GEOS-Chem by regridding it to the model resolution, here $0.5° \times 0.667°$, and (where needed) translating the RETRO species to the corresponding GEOS-Chem tracers (see Tables 2 and S1). The resulting annual global fluxes for anthropogenic VOCs emitted in GEOS-Chem are shown in Table S1 and Figure S1. We use the most recent RETRO data (year-2000) for all ensuing years, with the understanding that US VOC emissions have changed significantly since that time [*Fortin et al.*, 2005; *Harley et al.*, 2006; *Warneke et al.*, 2012; *McDonald et al.*, 2013]. RETRO emissions of $C_6$–$C_8$

**Table 3.** Seasonal Mixing Ratios (pptv) of Benzene, Toluene, and $C_8$ Aromatics Measured at the KCMP Tall Tower

| | Spring[a] | | Summer[b] | | Autumn[c] | | Winter[d] | |
|---|---|---|---|---|---|---|---|---|
| | Mean (Standard Deviation) | Median ($10^{th}$–$90^{th}$ Percentiles) | Mean (Standard Deviation) | Median ($10^{th}$–$90^{th}$ Percentiles) | Mean (Standard Deviation) | Median ($10^{th}$–$90^{th}$ Percentiles) | Mean (Standard Deviation) | Median ($10^{th}$–$90^{th}$ Percentiles) |
| Benzene | 89 (46) | 83 (35–145) | 48 (23) | 43 (24–78) | 80 (42) | 76 (29–131) | 160 (44) | 152 (115–214) |
| Toluene | 35 (42) | 23 (6–76) | 38 (36) | 29 (6–85) | 58 (52) | 45 (15–109) | 96 (65) | 79 (42–165) |
| $C_8$ aromatics | 54 (52) | 39 (13–108) | 77 (56) | 61 (26–158) | 99 (81) | 79 (34–181) | 125 (101) | 95 (42–239) |

[a]Spring: March to May.
[b]Summer: June to August.
[c]Autumn: September to November.
[d]Winter: December to February.

aromatic VOCs together account for ~23% of the total global anthropogenic VOC flux in GEOS-Chem on a carbon basis (16 TgC versus 71 TgC; Table S1 and Figure S1). Annual RETRO emissions over the contiguous US in RETRO are 420, 1448, and 2009 GgC/y for benzene, toluene, and $C_8$ aromatic compounds, respectively (Table 2). According to RETRO, US emissions account for approximately 25% of the total global source of these compounds for the year 2000 (Table 2).

The EPA NEI08 is a regional emission inventory covering the United States (http://www.epa.gov/ttn/chief/net/2008report.pdf). For this work, the NEI08 data have been processed using the 2008 EPA SMOKE platform (http://cmascenter.org/smoke/) based on the CB05 chemical mechanism [*Yarwood et al.*, 2005] with 12 km × 12 km spatial resolution and hourly temporal resolution, and regridded to the native GEOS-Chem resolution (here 0.5° × 0.667°) for years 2006 and 2010. Emissions for years other than 2006 or 2010 are scaled uniformly according to the EPA's published trend data (http://www.epa.gov/ttn/chief/trends/index.html). The resulting a priori year-2011 annual emissions over the contiguous US are 187 GgC benzene, 961 GgC toluene, and 865 GgC $C_8$ aromatic compounds, or 45%, 66%, and 43% of the corresponding RETRO estimates for year-2000. Figure 1 shows the annual mean surface mixing ratios of benzene, toluene, and $C_8$ aromatics predicted by GEOS-Chem based on NEI08.

In this paper, we use RETRO to estimate VOC emissions outside of the US when constructing the boundary conditions for our nested simulations. We then carry out separate analyses with US emissions computed using both RETRO and NEI08 inventories, as a way to test the sensitivity of our findings to the a priori emission assumptions. The RETRO and NEI08 inventories differ in a number of important respects (aside from geographic extent), including spatial and temporal resolution, speciation assumptions (Table 2), and the relative importance attributed to various source sectors. For example, on-road (vehicle road transportation) versus non-road (all other anthropogenic emissions) source partitioning differs significantly between the two inventories in the case of benzene (50% on-road in RETRO versus 29% in the NEI08) but is similar for toluene and $C_8$ aromatics (see section 8). In addition, RETRO extends only to year-2000, whereas the implementation of NEI08 used here predicts emissions for our specific years of analysis (2010 and 2011). Thus post-2000 emission changes in the US due to vehicle fleet changeover and other factors [*Fortin et al.*, 2005; *Harley et al.*, 2006; *Warneke et al.*, 2012; *McDonald et al.*, 2013] will in principle be accounted for in the NEI08, but not in the RETRO simulations.

## 3. Measured and Simulated Aromatic Mixing Ratios at the KCMP Tall Tower

Figure 2 shows hourly average mixing ratios of benzene, toluene, and $C_8$ aromatics measured at the KCMP tall tower during 2011. Annual mean measured mixing ratios were 91 pptv for benzene, 57 pptv for toluene, and 90 pptv for $C_8$ aromatics (see Table 3). We see in the data a pronounced seasonal cycle, with higher values in winter and lower values in summer (Figure 2 and Table 3), mainly reflecting the combined influence of seasonal changes in atmospheric OH and mixing depths. Figure 2 also shows simulated concentrations from GEOS-Chem based on the NEI08 emission inventory (corresponding plots for the RETRO inventory are shown in Figure S2).

While the GEOS-Chem simulation is able to capture the general annual patterns seen in the observations, some clear seasonally dependent biases emerge. Our base-case simulation using the NEI08 emission

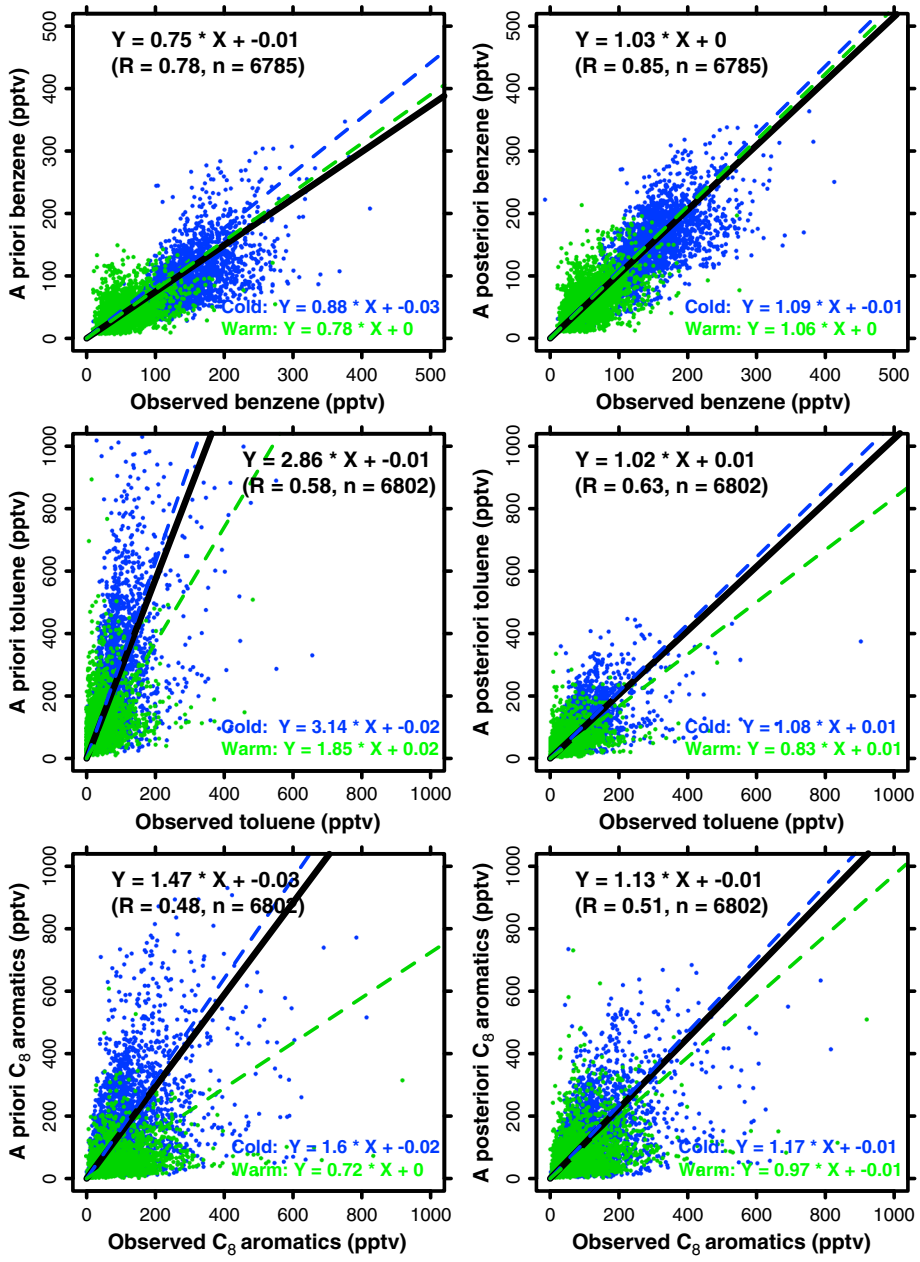


**Figure 3.** Atmospheric aromatic mixing ratios at the KCMP tall tower in 2011. The (left) GEOS-Chem a priori (based on NEI08) and (right) best-estimate a posteriori simulations are compared to measured values at the tall tower in 2011, colored by warm and cold seasons. Solid and dashed lines show the corresponding major axis fits, with regression parameters given inset (95% confidence intervals for slopes are better than ±5%, ±10%, and ±11% for benzene, toluene, and $C_8$ aromatics, respectively). Data points are 1 h mean values.

inventory overpredicts the observed toluene mixing ratios by a factor of 2–3 throughout the year (Figure 3). On the other hand, the model underpredicts the abundance of benzene and $C_8$ aromatics during the warm season (April to September) by 25%. During the cold season (October to March), the model has a consistent low bias for benzene (~40 pptv) while overpredicting $C_8$ aromatics by >60% (Figure 3).

The GEOS-Chem simulation based on the year-2000 RETRO emission inventory is shown in Figures S2 and S3. Here, the KCMP tall tower observations reveal a substantial high bias in the model for all aromatic species throughout the year. The annual model : measurement slopes (reduced major axis) in this case are 1.6 [95% confidence interval: 1.5–1.7], 3.9 [3.7–4.2], and 2.8 [2.6–3.0] for benzene, toluene, and $C_8$ aromatics, respectively, reflecting a RETRO overestimate of aromatic hydrocarbon emissions for the region sampled by the KCMP tall tower.

## 4. Optimizing Aromatic VOC Emissions Based on the Tall Tower Measurements

Using a Bayesian inverse approach, we use the above comparisons to derive optimized $C_6$–$C_8$ aromatic emission estimates that are most consistent with observational constraints (here the KCMP tall tower measurements) and with existing bottom-up information (the a priori emission inventories described in section 2.3). The procedure involves minimizing the scalar cost function $J(\mathbf{x})$ [*Rodgers*, 2000]:

$$J(\mathbf{x}) = (\mathbf{x} - \mathbf{x}_a)^T \mathbf{S}_a^{-1} (\mathbf{x} - \mathbf{x}_a) + (\mathbf{Kx} - \mathbf{y})^T \mathbf{S}_\Sigma^{-1} (\mathbf{Kx} - \mathbf{y}) \quad (1)$$

Here $\mathbf{x}$ is the vector of sources being optimized, while $\mathbf{x}_a$ represents their initial guess (a priori) values. $\mathbf{Kx}$ is the vector of predicted $C_6$–$C_8$ aromatic VOC mixing ratios at the KCMP tall tower and $\mathbf{y}$ is the corresponding vector of observations. $\mathbf{S}_a$ and $\mathbf{S}_\Sigma$ are the a priori and observational error covariance matrices, respectively. The minimum value of $J(\mathbf{x})$ thus defines the set of aromatic emissions that minimizes the error-weighted mismatch between the derived sources and their a priori values (first term on the right-hand side of equation (1)), plus the error-weighted mismatch between the tall tower data and the model predictions (the second term). $\mathbf{K}$ is the Jacobian matrix describing the forward model relationship between emissions and concentrations. In order to construct the Jacobian matrix $\mathbf{K}$, we perturb each model source individually by 10%, rerun the model, and calculate the resulting changes to the aromatic mixing ratios at the KCMP tall tower.

Errors in the a priori emissions are set initially at 100%, based on the US inventory biases inferred in other recent studies [*Parrish*, 2006; *Warneke et al.*, 2007; *Pétron et al.*, 2012]. Errors for different source sectors (e.g., on-road and non-road in the NEI08) are assumed uncorrelated so that $\mathbf{S}_a$ is diagonal. The observational error includes contributions from the measurements and from the model. Measurement uncertainties are estimated at 10%, 20%, and 10% for benzene, toluene, and $C_8$ aromatics, respectively (section 2.1). The model error is estimated at 20% following *Hu et al.* [2013] and *Kim et al.* [2013]. These relative uncertainties are applied to the measured and simulated concentrations accordingly, and the results added in quadrature to construct $\mathbf{S}_\Sigma$. We also derive alternate estimates of $\mathbf{S}_a$ and $\mathbf{S}_\Sigma$ based on a maximum likelihood estimation (MLE) approach, which infers the most probable elements of $\mathbf{S}_a$ and $\mathbf{S}_\Sigma$ based on the observed and (a priori) simulated $C_6$–$C_8$ aromatic mixing ratios [*Michalak et al.*, 2005]. Later, we test the dependence of our optimization results on the above assumptions and methods for constructing the error covariance matrices.

Our analyses first assessed which source combinations could be resolved based on the KCMP tall tower observations (on an annual basis). When using the NEI08 inventory, we find that on-road emissions, non-road emissions, and the model boundary condition (i.e., the influence of long-range transport from outside the model domain) can each be independently distinguished: the corresponding averaging kernel elements exceed $>0.95$ in each instance. Conversely, when using the RETRO inventory as the a priori estimate of US emissions, the on-road and non-road sectors cannot be distinguished as they are highly correlated in this inventory ($R > 0.98$). We thus combine them as a single state vector element to be optimized in this case. The fact that the tall tower data allows us to resolve on-road versus non-road sources when using NEI08 but not RETRO reflects the differing spatial distribution of these sectors between the two inventories.

In addition to the annual analysis, we perform separate optimizations on a two-season (cold = October to March; warm = April to September) or three-season (cold = December to February; warm = June to August; shoulder = March to May + September to November) basis to test for any seasonally dependent bias in the inventories. We find that toluene and the $C_8$ aromatics exhibit weak sensitivity to the model boundary condition during the warm season (averaging kernel values are $<0.3$), due to their short atmospheric lifetimes. Accordingly, we do not attempt to optimize the seasonal boundary condition for these compounds during the warm season (Table S2). In the following, we employ as our base-case analysis the semi-annual inversion with NEI08 as the a priori emission inventory (Opt1 in Table S2). Along with the separate annual and seasonal inversions, and those based on the RETRO inventory, we conduct an ensemble of sensitivity inversions (described in section 7) with varying model configurations and assumptions in order to test the robustness of our results.

## 5. Optimization Results

Our inversion results reveal a major overestimate of 2010–2011 toluene emissions in both the NEI08 (3× too high) and RETRO (4.5×) inventories. This finding is similar to that of *Warneke et al.* [2007], who inferred that an earlier version of NEI (NEI99) overpredicted toluene emissions in New England by nearly a factor of 3. In the

**Table 4.** Emission Correction Factors for the Best-Estimate Optimization Relative to the EPA's NEI08 Inventory[a]

| | Benzene | | | Toluene | | | $C_8$ aromatics | | |
|---|---|---|---|---|---|---|---|---|---|
| NEI08 (Opt1) | Non-road[b] | On-road[c] | Boundary Condition[d] | Non-road[b] | On-road[c] | Boundary Condition[d] | Non-road[b] | On-road[c] | Boundary Condition[d] |
| Cold[e] | 1.07 (0.84–1.44) | 0.75 (0.73–0.93) | 2.69 (2.21–3.53) | 0.17 (0.04–0.2) | 0.57 (0.55–0.64) | 1.85 (1.65–1.89) | 0.40 (0.11–0.57) | 1.23 (1.11–1.32) | 3.86 (3.40–4.03) |
| | 0.97[f] | | | 0.40[f] | | | 0.66[f] | | |
| Warm[g] | 0.97 (0.86–1.77) | 1.93 (1.87–2.06) | 2.80 (2.17–4.02) | 0.14 (0.06–0.22) | 1.02 (0.92–1.11) | — | 0.90 (0.48–1.10) | 2.23 (2.09–2.36) | — |
| | 1.23[f] | | | 0.45[f] | | | 1.23[f] | | |

[a]Uncertainty ranges from sensitivity tests are shown in parentheses.
[b]Non-road emissions: all anthropogenic sources except on-road transportation.
[c]On-road emissions: vehicle road transportation.
[d]Model boundary condition, reflecting sources upwind of North America.
[e]Cold season: October to March.
[f]The aggregated scale factors for the total US emission source in each season according to the best-estimate optimization.
[g]Warm season: April to September.

case of NEI08, part of the discrepancy found here can be attributed to speciation differences between CB05 (used to construct the emission fields) and GEOS-Chem, as the CB05 toluene tracer also includes ethylbenzene (Table 2). However, we find that this only increases the toluene flux by ~43% nationally and so cannot explain the observed disparity. Rather, the inferred toluene bias is primarily due to an overprediction of non-road emissions: a posteriori scale factors based on NEI08 are 0.17 [0.04–0.20] during the cold season and 0.14 [0.06–0.22] during the warm season for the non-road flux (numbers in brackets give the range from sensitivity tests described in section 7; see Table 4). On the other hand, our derived on-road emission estimates for toluene are more similar to the NEI08 values, with a posteriori scale factors of 1.02 [0.92–1.11] during the warm season and 0.57 [0.55–0.64] during the cold season. Our findings thus reverse the relative importance of on-road and non-road toluene emissions: non-road emissions account for 73% (NEI08) to 78% (RETRO) of the annual domestic toluene flux in the prior inventories, compared to 49% in our best-estimate optimization based on the tall tower data.

Our total derived emission sources for benzene and $C_8$ aromatics agree well with the NEI08; aggregated scale factors for US anthropogenic emissions are 1.10–1.23 (benzene) and 1.12–1.22 ($C_8$ aromatics) during the warm season, and 0.80–0.97 (benzene) and 0.66–0.88 ($C_8$ aromatics) during the cold season (Table 4). However, the optimization does reveal some significant season- and source-specific biases. We find that on-road emissions for benzene and $C_8$ aromatics are underestimated in the NEI08 by as much as a factor of 2 during the warm season (Table 4), with a posteriori scale factors of 1.93 [1.87–2.06] for benzene and 2.23 [2.09–2.36] for $C_8$ aromatics. However, this bias is not present during the cold season, when the optimized fluxes are within 25% of the prior NEI08 values (Table 4). There thus appears to be a seasonal bias in the NEI08 on-road emissions of benzene and $C_8$ aromatics, at least for the US Upper Midwest region sampled by the KCMP tall tower.

The non-road sector accounts for most of the US benzene and $C_8$ aromatic source in the prior NEI08 inventory, and this is also the case with our optimized emissions. Our derived non-road emissions for benzene agree with the NEI08 estimates: a posteriori scale factors are 1.07 [0.84–1.44] and 0.97 [0.86–1.77] during the cold and warm season, respectively. The corresponding scale factors for $C_8$ aromatics are 0.40 [0.11–0.57] during the cold season and 0.90 [0.48–1.10] during the warm season, suggesting an inventory overestimate for non-road emissions of $C_8$ aromatics during winter.

Employing RETRO as the a priori inventory within the US results in scale factors ranging from 0.35 to 0.50 for benzene and $C_8$ aromatics (Table S3), reflecting a twofold to threefold source overestimate for these compounds. As we see later, the a posteriori fluxes that we derive are consistent regardless of whether NEI08 or RETRO is used as a priori.

Aromatic VOC emissions outside the US are computed based on RETRO for our base-case simulation, as well as for all the sensitivity analyses described in section 7. In all cases, the optimizations reveal a large model underestimate of the $C_6$–$C_8$ aromatic abundance upwind of the US, with a posteriori scale factors of 2.03–4.02

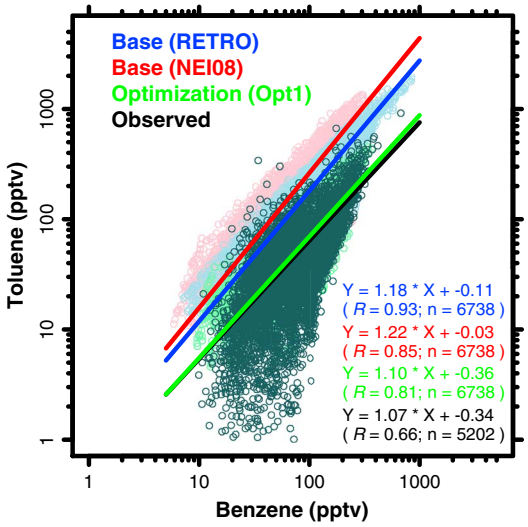


**Figure 4.** Relationship between benzene and toluene at the KCMP tall tower. Data are plotted on a log-log scale, with observations in black, a priori simulations in blue and red, and the best-estimate a posteriori in green. Solid lines show the corresponding major axis fits with regression parameters given inset. In the case of the observations, the regression slope and intercept are sensitive to the treatment of toluene data near the PTR-MS detection limit, estimated at 15–25 pptv. The parameters in the figure are derived based on a 20 pptv threshold; using 15 or 25 pptv changes the slope by ±5% (1.03 to 1.13) and the intercept by ±35% (−0.24 to −0.46). Toluene measurements below the detection limit of 20 pptv represent 24% of the total data. X and Y in the regression equations given inset correspond to $\log_{10}$(benzene) and $\log_{10}$(toluene).

for benzene, 1.65–2.14 for toluene, and 3.40–4.92 for $C_8$ aromatics. This may reflect a significant emission bias over East Asia, at least in the case of benzene, which has a sufficiently long lifetime to undergo substantial long-range transport. *Liu et al.* [2012] concluded on the basis of space-borne glyoxal measurements that Chinese aromatic emissions are 6 times greater than the bottom-up estimate of *Zhang et al.* [2009].

Figure 3 compares the mixing ratios of benzene, toluene, and $C_8$ aromatics observed at the KCMP tall tower during 2011 with those from our base-case a priori and best-estimate a posteriori simulations (using the NEI08 inventory). For all species, we see improved model : observation agreement with the a posteriori simulation, as indicated by higher correlation coefficients ($R$; 0.85 versus 0.78, 0.63 versus 0.58, and 0.51 versus 0.48, for benzene, toluene, and $C_8$ aromatics) and slopes closer to one (1.03 versus 0.75, 1.02 versus 2.88, and 1.13 versus 1.47, respectively) compared to the a priori simulation. In general, we see a major revision for toluene, and more modest adjustments for $C_8$ aromatics and for benzene. The seasonal model : observation regression slopes are also greatly improved in the a posteriori simulation. We derive similar a posteriori model-observation comparisons when using RETRO as the a priori inventory (Figure S3).

A feature of the regressions in Figures 3 and S3 is that the model : observation correlation coefficients increase with the lifetime of species at hand (e.g., $R = 0.51$ for $C_8$ aromatics versus 0.85 for benzene in our best-estimate a posteriori simulation based on NEI08). This mainly reflects model difficulty in capturing fine-scale processes (e.g., spatially heterogeneous emissions, chemistry, and mixing effects) that become increasingly important for shorter-lived species. The fact that the optimized simulation substantially improves the model : observation slopes in each case, while only moderately increasing the correlation coefficients, suggests (i) that the overall biases in the model emissions are mostly corrected in the a posteriori simulations and (ii) that significantly improving the model : observation correlation would require improved representations of other model processes.

Figure 4 compares the observed benzene : toluene relationship with that in the a priori and a posteriori simulations. Such aromatic hydrocarbon:hydrocarbon relationships have been widely used to diagnose atmospheric photochemistry and transport/dilution [e.g., *McKeen and Liu*, 1993; *McKeen et al.*, 1996], since both species are generally coemitted directly from similar sources but then undergo photochemical loss at differing rates. As shown in Figure 4, our best-estimate optimization (Opt1) clearly captures the observed benzene : toluene relationship, while two a priori simulations fail to do so. The improvement is largely due to modification of the benzene: toluene emission ratio: the total US emission ratio for benzene:toluene is 0.50 GgC/GgC in the best-estimate optimization, versus 0.19 in NEI08, and 0.30 in RETRO (see section 8 and Figure 7).

## 6. Source Contributions to Atmospheric Aromatics in the US Upper Midwest

Figure 5 shows the seasonal contribution from long-range transport (i.e., the nested model boundary condition), domestic on-road sources, and non-road sources for benzene, toluene, and $C_8$ aromatics at the KCMP tall tower according to our best-estimate optimization.

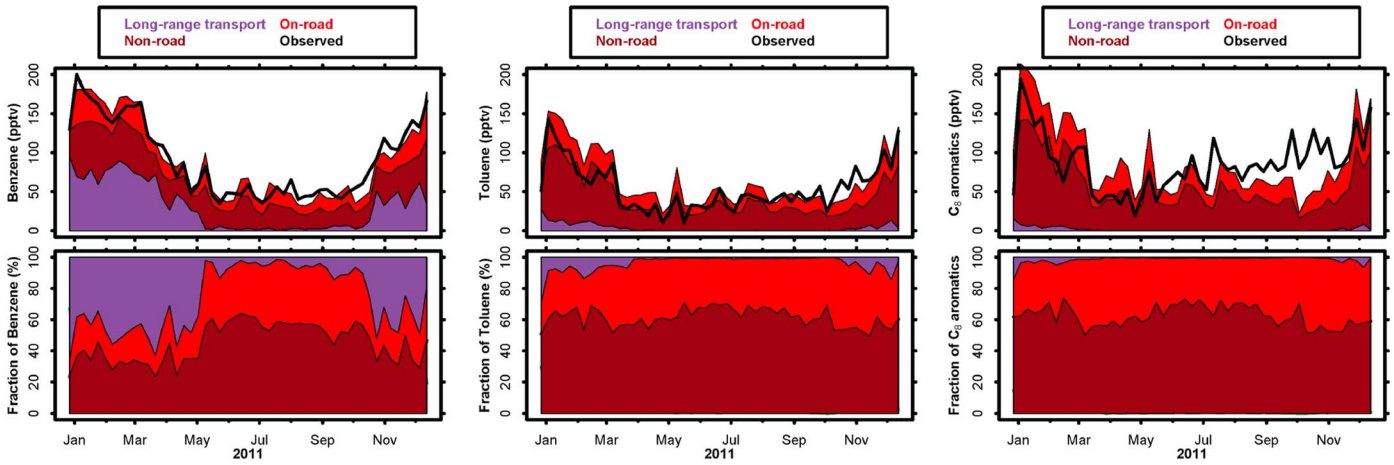


**Figure 5.** Seasonal source contributions to mixing ratios of (left) benzene, (middle) toluene, and (right) $C_8$ aromatics at the KCMP tall tower. Top rows show stack plots of the seasonal mixing ratios (weekly mean) based on the best-estimate GEOS-Chem a posteriori simulation. Also shown are the observed mixing ratios at the tall tower (black lines). Bottom rows show the fractional contribution of these sources to the total modeled aromatic abundance in the optimized simulation.

We find that long-range transport is a major contributor to atmospheric benzene during winter in the Upper Midwest, accounting for up to 56% of the total abundance at that time of year (mean of 43%). This arises as a direct consequence of the large upward adjustment to the model boundary condition that is indicated by the tall tower data and which is a common feature of all the sensitivity tests. The influence of long-range transport on wintertime mixing ratios of toluene (up to 14%, mean of 8%) and $C_8$ aromatics (up to 6%, mean of 3%) is more modest as a result of their shorter atmospheric lifetimes.

In terms of domestic aromatic sources, our best-estimate optimization (Opt1) finds that on-road mobile emissions are comparable in importance to non-road emissions for all $C_6$–$C_8$ aromatic compounds during the warm season (Figure 5 and Table S2). During the cold season, on-road emissions of benzene and toluene decrease from their warm-season values (Table S2), and non-road emissions become relatively more important (Table S2 and Figure 5). In the case of $C_8$ aromatics, both non-road and on-road emissions are lower in the cold season than in the warm season according to the optimization.

## 7. Uncertainty Analysis

The best-estimate optimization described above is performed on a semiannual basis (warm season/cold season), with NEI08 as the prior US emission inventory and with the forward and inverse model configured as described in sections 2.3 and 4. In this section, we repeat the optimization while varying a number of key forward model parameters, error estimates, and observation selection criteria in order to obtain a comprehensive uncertainty estimate for our results (Table S2). This includes (1) use of differing a priori inventories (NEI08 and RETRO) for US aromatic VOC emissions; (2) including and excluding bromine chemistry, which modifies the model distribution of OH and $O_3$ as described by *Parrella et al.* [2012]; (3) varying the reactive uptake coefficient for $HO_2$ on aqueous aerosols ($\gamma = 0.2$ or 0.4), which modifies the global $HO_x$ fields in the model [*Mao et al.*, 2013]; (4) including and excluding dry deposition for aromatic VOCs, and also including and excluding reactive uptake for these compounds [*Karl et al.*, 2010]; (5) use of two alternative boundary layer mixing schemes (local and nonlocal; [*Holtslag and Boville*, 1993; *Lin and McElroy*, 2010]); (6) decreasing $NO_x$ emissions over North America by 40% [*Russell et al.*, 2012]; (7) alternate assumptions for the error covariance matrices: (i) doubling and halving $\mathbf{S}_a$, (ii) doubling and halving $\mathbf{S}_\Sigma$, and (iii) constructing $\mathbf{S}_a$ and $\mathbf{S}_\Sigma$ using Maximum Likelihood Estimation [*Michalak et al.*, 2005]; and (8) varying the time frame and temporal resolution of the optimization: (i) annual inversion for 2010, (ii) annual inversion for 2011, (iii) annual inversion for 2010 + 2011, (iv) two-season inversion (cold/warm) for 2011, and (v) three-season inversion (cold/warm/shoulder) for 2011.

Table S2 shows results from the resulting 25 sensitivity inversions. These sensitivity runs may not span every single possible cause of error in the analysis, but they do serve to assess the main sources of uncertainty and

their relative magnitudes. We find that doubling or halving the a priori error covariance matrix ($\mathbf{S}_a$) does not change the emission estimates by >1%, so this test is not included in Table S2.

In a relative sense, we find that the total and on-road emissions for each species (benzene, toluene, $C_8$ aromatics) are better quantified than the contribution from non-road sources. For each species, the inferred on-road vehicle emissions vary by only ~30% across all the sensitivity inversions, whereas the inferred non-road emissions differ by up to 70% (Table S2). The KCMP tall tower footprint thus provides a somewhat stronger constraint for on-road than for non-road sources of aromatics. Across all the sensitivity runs, the derived total emissions all fall within ±50% of our best-estimate optimization (Opt1) for benzene, toluene, and $C_8$ emissions.

The suite of test inversions summarized in Table S2 indicates that our derived emissions are most sensitive to the assumptions used to construct $\mathbf{S}_\Sigma$ (e.g., Opt6–Opt9) and to model treatment of reactive uptake (e.g., Opt16–Opt17). Here, the inferred non-road and total emissions diverge by as much as ~70% and ~50%, respectively, from the best estimate, and the inferred on-road source varies by up to ~30%. By comparison, use of alternate prior inventories (NEI08 versus RETRO), different PBL mixing schemes, and perturbations to model chemistry (40% decrease in US $NO_x$ emissions; changing the reactive uptake efficiency for $HO_2$; including bromine chemistry) all have a much smaller influence on the results, with discrepancies of less than 25% compared to the best estimate.

An inherent bias in our a priori NEI08 emissions arises from speciation differences between that inventory and GEOS-Chem (Table 2). The NEI08 inventory used in our best-estimate analysis is based on CB05 speciation [*Yarwood et al.*, 2005], which lumps other monoalkyl aromatics with toluene, and other polyalkyl aromatics with $C_8$ aromatics. By contrast, the PTR-MS measurements resolve VOCs based on their mass, so that all $C_8$ aromatics (xylenes + ethylbenzene) are measured together while benzene and toluene are detected as individual compounds. The chemical mechanism employed in GEOS-Chem for this work corresponds to this latter speciation. We performed an analysis to quantify the expected bias in the NEI08 a priori toluene and $C_8$ aromatic emissions due to this discrepancy. We find that, nationally, emissions of the lumped CB05 TOLU tracer (toluene + ethlybenzene) are ~43% higher than those of toluene itself, while emissions of the lumped CB05 XYLE tracer (xylenes + other polyalkyl aromatics) are 25% higher than those of $C_8$ aromatics alone. These speciation differences will also vary spatially and between sectors. However, even the largest sector-specific a priori speciation biases (e.g., a priori non-road TOLU emissions in the NEI08 are ~2.2 times those of toluene itself) are substantially smaller than the corresponding top-down correction factors derived here (e.g., an inferred 4.5 to 16 times reduction of toluene non-road emissions). As shown above, our a posteriori flux estimates are not sensitive to the choice of prior inventory nor to its assigned error covariance; this speciation discrepancy can therefore be expected to bias the NEI08 a priori emission estimates for toluene and $C_8$ aromatics, but should not notably affect the a posteriori results.

## 8. Aircraft Comparisons and Implications for Aromatic VOC Emissions in the United States

An implicit assumption in the above optimizations is that the spatial distribution of each individual emission sector is described accurately in the prior inventories. As seen earlier, however, there is some spatial disparity between RETRO and NEI08, indicating a degree of uncertainty in this regard. In this section, we test the extent to which aromatic emission corrections inferred from the KCMP tall tower measurements apply more broadly across the contiguous US. To this end, we employ recent aircraft measurements covering six key regions across the US: California (CALNEX, DISCOVER-AQ California), US East Coast (DISCOVER-AQ Baltimore-Washington, DC), Central US (DC3), US Southeast (SENEX), and Texas (DISCOVER-AQ Texas); see Table 1 and Figure 1.

Figure 6 compares the median vertical profiles of benzene and toluene for each of these campaigns (in black) with our base-case a priori (NEI08; red) and best-estimate a posteriori (green, Opt1) simulations. Corresponding plots for simulations using RETRO as the a priori US inventory are shown in Figure S4. The comparisons for $C_8$ aromatics are plotted in Figure S5. Model simulations are for the year 2011, whereas the aircraft campaigns span 2010-2013. However, we expect year-to-year emission changes over this time period to be within the overall uncertainty in our analysis (section 7). All simulations are sampled along the flight

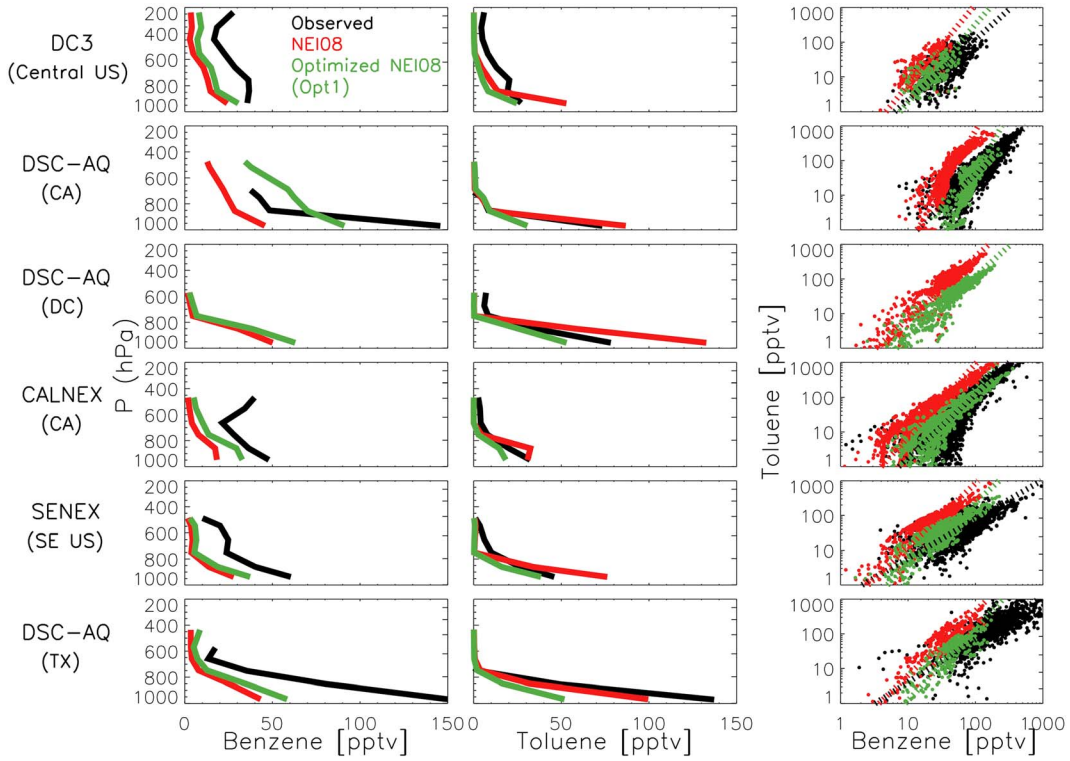


**Figure 6.** Vertical distribution of benzene and toluene over North America. (left and middle) Median vertical profiles of benzene and toluene observed (black) and simulated by GEOS-Chem based on NEI08 (red: base-case a priori; green: best-estimate optimization) during six recent aircraft campaigns. (right) Boundary layer ($P > 800$ hPa) benzene-toluene relationships for the same aircraft campaigns with dashed lines showing the best fits from major axis regression. DSC-AQ (CA): DISCOVER-AQ California; DSC-AQ (DC): DISCOVER-AQ Baltimore-Washington, DC; DSC-AQ (TX): DISCOVER-AQ Texas.

tracks at the time-of-day and day-of-year of the observations, and airborne data have been filtered to remove the influence of individual biomass burning plumes (acetonitrile > 200 pptv).

For benzene, we see in Figure 6 a general increase in the simulated mixing ratios with the best estimate a posteriori simulation and improved model : measurement agreement (to varying degree) across all the aircraft campaigns. Note that the S-shape seen in the measured DC3 profile is due to targeted sampling of convection during that study; the model simulation is for a different year and does not capture such effects. The model still appears too low compared to the observations within the atmospheric boundary layer (in particular for DISCOVER-AQ California and Texas), though the bias is reduced. The two main factors contributing to this shift are (i) the nearly doubling (scale factor = 1.93) of the on-road benzene emissions during the warm season when five of the six campaigns were carried out and (ii) the large inferred increase (2–3 times) in the model boundary condition, reflecting long-range transport of benzene into North America. The latter is important only in winter, when the benzene lifetime increases to several months.

In the case of toluene, our inferred ~85% reduction for non-road emissions (a posteriori scale factors of 0.17 and 0.14 during the cold and warm season, respectively) strongly improves the model : measurement agreement over most areas of the US (Central, East, and Southeastern), with the two notable exceptions of California and Houston, Texas (CALNEX, DISCOVER-AQ California, DISCOVER-AQ Texas; Figure 6). In these locations, a priori toluene emissions based on NEI08 appear to be more reliable than our a posteriori result, highlighting very large non-road emissions in these areas that may be related to petroleum refineries and petrochemical facilities.

In the case of the RETRO simulations for benzene, we actually see degraded model-measurement agreement in the a posteriori for every aircraft campaign but one (CALNEX; Figure S4). This discrepancy reflects the spatial disparities between RETRO and NEI08 discussed earlier, which may be partially due to regionally specific changes between 2000 and 2010–2011. We note that the a priori NEI08 simulation has a much

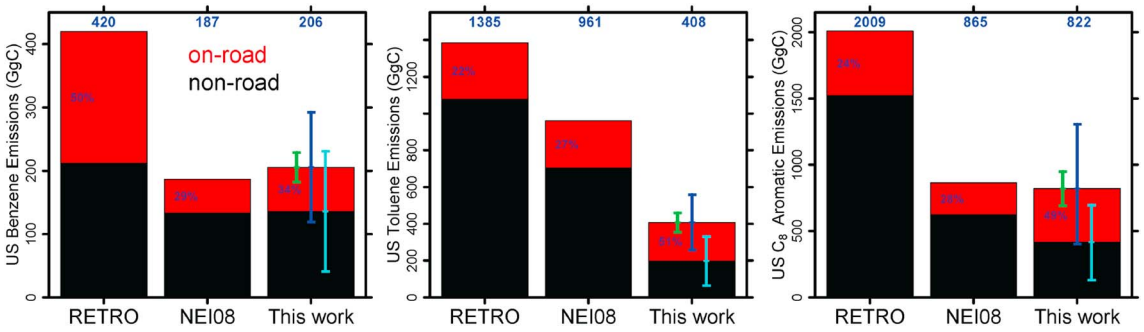


**Figure 7.** Annual aromatic emissions in the contiguous US in the RETRO (for year-2000) and NEI08 (for year-2011) a priori emission inventories, compared to our best-estimate a posteriori emissions. Also shown are the fractional contribution from on-road emissions (percentages given in red portion of the bars) and the total emissions in GgC (blue numbers above each bar) in the a posteriori estimate. Uncertainty ranges from 25 sensitivity runs (Table S2) are shown for the a posteriori total emissions (blue error bars), on-road emissions (green), and non-road emissions (cyan).

stronger correlation with the tall tower observations than does the a priori RETRO simulation ($R = 0.78$ versus $R = 0.54$), suggesting a superior representation of the spatial distribution of benzene emissions in 2010–2011 for the NEI08 compared to RETRO. On the other hand, for toluene the a posteriori simulation based on RETRO is in good agreement with the aircraft data for all locations except Houston, Texas. As seen earlier for the tall tower data, in all cases the observed benzene : toluene relationships are much better captured by the best-estimate a posteriori simulation than by the a priori (right panels in Figures 6 and S4).

Based on the comparisons above, we conclude that the benzene biases inferred from the KCMP tall tower measurements are generally present across the EPA's NEI08 inventory within the contiguous US. The same is not true for RETRO, which clearly has benzene biases that vary regionally in a significant way. For both inventories, our inferred emission biases for toluene appear to be applicable to most areas of the contiguous US, with clear exceptions in California and Texas. For $C_8$ aromatic emission (Figure S5), the inferred NEI08 and RETRO emission biases also appear to apply to most areas of the contiguous US.

Applying the emission scale factors from our best-estimate optimization based on NEI08 (Opt1 in Table S2) and using the a priori toluene emissions for CA and TX, we estimate total anthropogenic emission fluxes in the contiguous US for 2011 of 206 GgC for benzene (with an uncertainty range from the 25 sensitivity runs of 180–297 GgC; Figure 7), 408 GgC for toluene (257–559 GgC), and 822 GgC for $C_8$ aromatics (403–1028 GgC). Annually, the best-estimate top-down values for benzene and $C_8$ aromatics agree well with our a priori emissions based on the EPA's NEI08 inventory, given the uncertainties of the analysis (Figure 7). However, toluene emissions are substantially overestimated in our a priori implementation of NEI08 (961 GgC in the a priori versus 408 GgC in our best-estimate a posteriori); the discrepancy is nearly a factor of three in most areas of the US except California and Texas. Figure 7 also shows that the fractional importance of on-road BTEX emissions is greater than assumed in the EPA NEI08 inventory.

In summary, we find that toluene emissions are significantly overestimated in our implementation of the EPA's NEI08 throughout the year for the upper Midwest region as well as the central and eastern US. The overestimate is mostly associated with non-road sources but is also partly due to speciation discrepancies between CB05 and GEOS-Chem (Figure 7 and Table 2). Our best-estimate optimization implies that on-road emissions of benzene and $C_8$ aromatics are underestimated by the EPA NEI08 inventory, particularly during the warm season (Table 4). This finding implies that tailpipe and fuel evaporative emissions are not accurately captured in current inventories. The doubling of the on-road flux of benzene and $C_8$ aromatics during the warm season that is implied by our optimization changes the seasonal cycle of emissions for these compounds, with slightly higher a posteriori emissions during the warm season than in the cold season (Figure 8 and Table 4). In general, we find that the seasonal and non-road contributions to BTEX emissions are less well constrained by the optimization (e.g., uncertainty ranges of ±70%, ±67%, and ±68% for non-road benzene, toluene, and $C_8$ aromatics, respectively) than are the on-road sources and the total flux (±51% or better; Table S2 and Figure 7).

We find that US $C_6$–$C_8$ aromatic emissions in the RETRO inventory are overestimated by factors of 2.0 (1.4–3.5; uncertainty range from sensitivity runs), 4.5 (3.3–7.1), and 2.4 (1.5–5.0) for benzene, toluene, and $C_8$ aromatics,

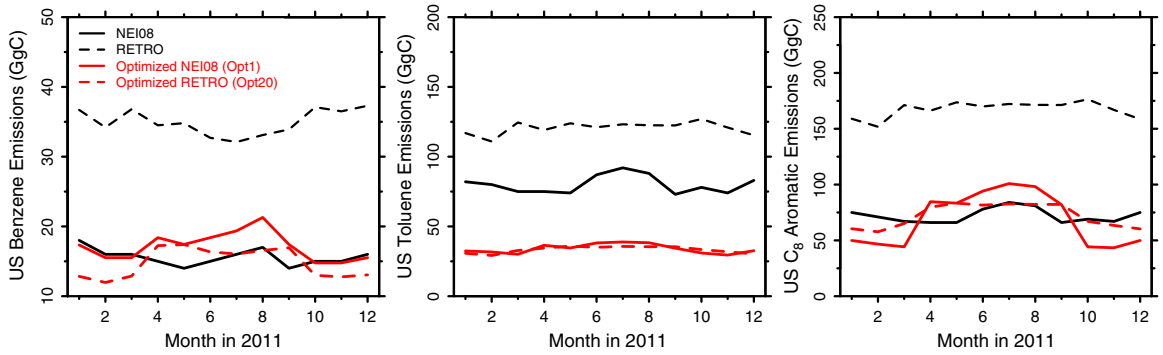


**Figure 8.** National monthly total emissions of (left) benzene, (middle) toluene, and (right) $C_8$ aromatics in the a priori NEI08 (black solid line) and RETRO (black dashed line) inventories, compared to the a posteriori estimates based on NEI08 (red solid line; Opt1 in Table S2) and RETRO (red dashed line; Opt20 in Table S2).

respectively. Part of this overestimate likely reflects the substantial anthropogenic VOC emission reductions that occurred in the US between 2000 (the most recent RETRO year used here) and 2010–2011. Regardless of whether the NEI or RETRO inventory is used as a priori over the US, we derive statistically identical a posteriori flux estimates (Figures 7 and 8).

In the future, sustained measurements are needed in other key regions of the US and elsewhere to (i) determine the reasons for the spatial and temporal sector emission biases seen in this and other studies [e.g., *Kopacz et al.*, 2010; *Stein et al.*, 2014], (ii) monitor future changes and the evolving importance of long-range transport for these compounds and other air pollutants in the US, and (iii) better quantify aromatic emissions and their trends in East Asia.

**Acknowledgments**

This study was supported by the National Science Foundation (grants 0937004 and 1148951), by the Minnesota Supercomputing Institute, and by a University of Minnesota Doctoral Dissertation Fellowship. We thank Tom Nelson and Minnesota Public Radio for their logistical support at the KCMP tall tower. PTR-MS measurements during DISCOVER-AQ and DC-3 were supported by the Austrian Space Applications Programme (ASAP, bmvit, FFG-ALR). TM was supported by the NASA Postdoctoral Program. We acknowledge the US Environmental Protection Agency for providing 2006 and 2010 North American emission inventories. These emission inventories are intended for research purposes and were developed for Phase 2 of the Air Quality Model Evaluation International Initiative (AQMEII) using information from the 2008-based modeling platform (http://www.epa.gov/ttn/chief/emch/index.html#2008) as a starting point. Measurements from the KCMP tall tower described here are available for download at http://www.atmoschem.umn.edu/data.htm.

## References

Ahmadov, R., et al. (2014), Understanding high wintertime ozone pollution events in an oil and natural gas producing region of the western US, *Atmos. Chem. Phys. Discuss.*, *14*(14), 20,295–20,343, doi:10.5194/acpd-14-20295-2014.

Akagi, S. K., R. J. Yokelson, C. Wiedinmyer, M. J. Alvarado, J. S. Reid, T. Karl, J. D. Crounse, and P. O. Wennberg (2011), Emission factors for open and domestic biomass burning for use in atmospheric models, *Atmos. Chem. Phys.*, *11*(9), 4039–4072, doi:10.5194/acp-11-4039-2011.

Andreae, M. O., and P. Merlet (2001), Emission of trace gases and aerosols from biomass burning, *Global Biogeochem. Cy.*, *15*(4), 955–966, doi:10.1029/2000GB001382.

Atkinson, R., D. Baulch, R. Cox, J. Crowley, R. Hampson, R. Hynes, M. Jenkin, M. Rossi, and J. Troe (2006), Evaluated kinetic and photochemical data for atmospheric chemistry: Volume II—Gas phase reactions of organic species, *Atmos. Chem. Phys.*, *6*(11), 3625–4055, doi:10.5194/acp-6-3625-2006.

Baan, R., et al. (2009), A review of human carcinogens—Part F: Chemical agents and related occupations, *Lancet Oncol.*, *10*(12), 1143–1144, doi:10.1016/S1470-2045(09)70358-4.

Baasandorj, M., D. B. Millet, L. Hu, D. Mitroo, and B. J. Williams (2014), Measuring acetic and formic acid by proton transfer reaction-mass spectrometry: Sensitivity, humidity dependence, and quantifying interferences, *Atmos. Meas. Tech. Discuss.*, *7*, 10,883–10,930, doi:10.5194/amtd-7-10883-2014.

Bar-Ilan, A., J. Grant, R. Friesen, A. Pollack, D. Henderer, D. Pring, and K. Sgamma (2008), Development of baseline 2006 emissions from oil and gas activity in the Denver-Julesburg Basin, WRAP Phase III report, Fort Collins, Colo.

Bey, I., D. J. Jacob, R. M. Yantosca, J. A. Logan, B. D. Field, A. M. Fiore, Q. Li, H. Y. Liu, L. J. Mickley, and M. G. Schultz (2001), Global modeling of tropospheric chemistry with assimilated meteorology: Model description and evaluation, *J. Geophys. Res.*, *106*(D19), 23,073–23,095, doi:10.1029/2001JD000807.

CDPHE (2008), Denver metropolitan area and North Front Range 8-hour ozone state implementation plan—Emissions inventory, Denver, Colo.

de Gouw, J. A., and C. Warneke (2007), Measurements of volatile organic compounds in the Earth's atmosphere using proton-transfer-reaction mass spectrometry, *Mass Spectrom. Rev.*, *26*(2), 223–257, doi:10.1002/mas.20119.

de Gouw, J. A., P. D. Goldan, C. Warneke, W. C. Kuster, J. M. Roberts, M. Marchewka, S. B. Bertman, A. A. P. Pszenny, and W. C. Keene (2003), Validation of proton transfer reaction-mass spectrometry (PTR-MS) measurements of gas-phase organic compounds in the atmosphere during the New England Air Quality Study (NEAQS) in 2002, *J. Geophys. Res.*, *108*(D21), 4682, doi:10.1029/2003JD003863.

Fortin, T. J., B. J. Howard, D. D. Parrish, P. D. Goldan, W. C. Kuster, E. L. Atlas, and R. A. Harley (2005), Temporal changes in U.S. benzene emissions inferred from atmospheric measurements, *Environ. Sci. Technol.*, *39*(6), 1403–1408, doi:10.1021/es049316n.

Griffis, T. J., J. M. Baker, S. D. Sargent, M. Eriksson, J. Corcoran, M. Chen, and K. Billmark (2010), Influence of $C_4$ vegetation on $^{13}CO_2$ discrimination and isoforcing in the Upper Midwest, United States, *Global Biogeochem. Cy.*, *24*, GB4006, doi:10.1029/2009GB003768.

Griffis, T. J., X. Lee, J. M. Baker, M. P. Russelle, X. Zhang, R. Venterea, and D. B. Millet (2013), Reconciling the differences between top-down and bottom-up estimates of nitrous oxide emissions for the U.S. Corn Belt, *Global Biogeochem. Cy.*, *27*, 746–754, doi:10.1002/gbc.20066.

Harley, R. A., D. S. Hooper, A. J. Kean, T. W. Kirchstetter, J. M. Hesson, N. T. Balberan, E. D. Stevenson, and G. R. Kendall (2006), Effects of reformulated gasoline and motor vehicle fleet turnover on emissions and ambient concentrations of benzene, *Environ. Sci. Technol.*, *40*(16), 5084–5088, doi:10.1021/es0604820.

Henze, D. K., J. H. Seinfeld, N. L. Ng, J. H. Kroll, T. M. Fu, D. J. Jacob, and C. L. Heald (2008), Global modeling of secondary organic aerosol formation from aromatic hydrocarbons: High- vs. low-yield pathways, *Atmos. Chem. Phys.*, *8*(9), 2405–2420, doi:10.5194/acp-8-2405-2008.

Holtslag, A., and B. Boville (1993), Local versus nonlocal boundary-layer diffusion in a global climate model, *J. Clim.*, *6*(10), 1825–1842.
Hu, L., D. B. Millet, M. J. Mohr, K. C. Wells, T. J. Griffis, and D. Helmig (2011), Sources and seasonality of atmospheric methanol based on tall tower measurements in the US Upper Midwest, *Atmos. Chem. Phys.*, *11*(21), 11,145–11,156, doi:10.5194/acp-11-11145-2011.
Hu, L., D. B. Millet, S. Y. Kim, K. C. Wells, T. J. Griffis, E. V. Fischer, D. Helmig, J. Hueber, and A. J. Curtis (2013), North American acetone sources determined from tall tower measurements and inverse modeling, *Atmos. Chem. Phys.*, *13*(6), 3379–3392, doi:10.5194/acp-13-3379-2013.
Jaars, K., et al. (2014), Ambient aromatic hydrocarbon measurements at Welgegund, South Africa, *Atmos. Chem. Phys.*, *14*(13), 7075–7089, doi:10.5194/acp-14-7075-2014.
Jacob, D. J., J. H. Crawford, M. M. Kleb, V. S. Connors, R. J. Bendura, J. L. Raper, G. W. Sachse, J. C. Gille, L. Emmons, and C. L. Heald (2003), Transport and chemical evolution over the Pacific (TRACE-P) aircraft mission: Design, execution, and first results, *J. Geophys. Res.*, *108*(D20), 9000, doi:10.1029/2002JD003276.
Johnson, D., M. E. Jenkin, K. Wirtz, and M. Martin-Reviejo (2005), Simulating the formation of secondary organic aerosol from the photooxidation of aromatic hydrocarbons, *Environ. Chem.*, *2*(1), 35–48, doi:10.1071/EN04079.
Kaiser, E. W., W. O. Siegl, D. F. Cotton, and R. W. Anderson (1992), Effect of fuel structure on emissions from a spark-ignited engine. 2. Naphthene and aromatic fuels, *Environ. Sci. Technol.*, *26*(8), 1581–1586, doi:10.1021/es00032a014.
Karl, T., E. Apel, A. Hodzic, D. D. Riemer, D. R. Blake, and C. Wiedinmyer (2009), Emissions of volatile organic compounds inferred from airborne flux measurements over a megacity, *Atmos. Chem. Phys.*, *9*(1), 271–285, doi:10.5194/acp-9-271-2009.
Karl, T., P. Harley, L. Emmons, B. Thornton, A. Guenther, C. Basu, A. Turnipseed, and K. Jardine (2010), Efficient atmospheric cleansing of oxidized organic trace gases by vegetation, *Science*, *330*(6005), 816–819, doi:10.1126/science.1192534.
Kim, S. Y., D. B. Millet, L. Hu, M. J. Mohr, T. J. Griffis, D. Wen, J. C. Lin, S. M. Miller, and M. Longo (2013), Constraints on carbon monoxide emissions based on tall tower measurements in the U.S. Upper Midwest, *Environ. Sci. Technol.*, *47*(15), 8316–8324, doi:10.1021/es4009486.
Kopacz, M., et al. (2010), Global estimates of CO sources with high resolution by adjoint inversion of multiple satellite datasets (MOPITT, AIRS, SCIAMACHY, TES), *Atmos. Chem. Phys.*, *10*(3), 855–876, doi:10.5194/acp-10-855-2010.
Levi, M. A. (2012), Comment on "Hydrocarbon emissions characterization in the Colorado Front Range: A pilot study" by Gabrielle Pétron et al, *J. Geophys. Res.*, *117*, D21203, doi:10.1029/2012JD017686.
Levi, M. A. (2013), Reply to "Reply to 'Comment on "Hydrocarbon emissions characterization in the Colorado Front Range – A Pilot Study"' by Michael A. Levi" by Gabrielle Pétron et al, *J. Geophys. Res. Atmos.*, *118*, 3044–3046, doi:10.1002/jgrd.50299.
Lin, J. T., and M. B. McElroy (2010), Impacts of boundary layer mixing on pollutant vertical profiles in the lower troposphere: Implications to satellite remote sensing, *Atmos. Environ.*, *44*(14), 1726–1739, doi:10.1016/j.atmosenv.2010.02.009.
Liu, Z., et al. (2010), Evidence of reactive aromatics as a major source of peroxy acetyl nitrate over China, *Environ. Sci. Technol.*, *44*(18), 7017–7022, doi:10.1021/es1007966.
Liu, Z., et al. (2012), Exploring the missing source of glyoxal (CHOCHO) over China, *Geophys. Res. Lett.*, *39*, L10812, doi:10.1029/2012GL051645.
Mao, J., et al. (2010), Chemistry of hydrogen oxide radicals ($HO_x$) in the Arctic troposphere in spring, *Atmos. Chem. Phys.*, *10*(13), 5823–5838, doi:10.5194/acp-10-5823-2010.
Mao, J., S. Fan, D. J. Jacob, and K. R. Travis (2013), Radical loss in the atmosphere from Cu-Fe redox coupling in aerosols, *Atmos. Chem. Phys.*, *13*(2), 509–519, doi:10.5194/acp-13-509-2013.
Martín-Reviejo, M., and K. Wirtz (2005), Is benzene a precursor for secondary organic aerosol?, *Environ. Sci. Technol.*, *39*(4), 1045–1054, doi:10.1021/es049802a.
McDonald, B. C., D. R. Gentner, A. H. Goldstein, and R. A. Harley (2013), Long-term trends in motor vehicle emissions in U.S. urban areas, *Environ. Sci. Technol.*, *47*(17), 10,022–10,031, doi:10.1021/es401034z.
McKeen, S. A., and S. C. Liu (1993), Hydrocarbon ratios and photochemical history of air masses, *Geophys. Res. Lett.*, *20*(21), 2363–2366, doi:10.1029/93GL02527.
McKeen, S. A., S. C. Liu, E. Y. Hsie, X. Lin, J. D. Bradshaw, S. Smyth, G. L. Gregory, and D. R. Blake (1996), Hydrocarbon ratios during PEM-WEST A: A model perspective, *J. Geophys. Res.*, *101*(D1), 2087–2109, doi:10.1029/95JD02733.
Michalak, A. M., A. Hirsch, L. Bruhwiler, K. R. Gurney, W. Peters, and P. P. Tans (2005), Maximum likelihood estimation of covariance parameters for Bayesian atmospheric trace gas surface flux inversions, *J. Geophys. Res.*, *110*, D24107, doi:10.1029/2005JD005970.
Millet, D. B., et al. (2004), Volatile organic compound measurements at Trinidad Head, California, during ITCT 2K2: Analysis of sources, atmospheric composition, and aerosol residence times, *J. Geophys. Res.*, *109*, D23S16, doi:10.1029/2003JD004026.
Millet, D. B., N. M. Donahue, S. N. Pandis, A. Polidori, C. O. Stanier, B. J. Turpin, and A. H. Goldstein (2005), Atmospheric volatile organic compound measurements during the Pittsburgh Air Quality Study: Results, interpretation, and quantification of primary and secondary contributions, *J. Geophys. Res.*, *110*, D07S07, doi:10.1029/2004JD004601.
Millet, D. B., et al. (2006), Chemical characteristics of North American surface layer outflow: Insights from Chebogue Point, Nova Scotia, *J. Geophys. Res.*, *111*, D23S53, doi:10.1029/2006JD007287.
Müller, M., et al. (2014), A compact PTR-ToF-MS instrument for airborne measurements of VOCs at high spatio-temporal resolution, *Atmos. Meas. Tech.*, *7*, 3763–3772, doi:10.5194/amt-7-3763-2014.
Murphy, J. G., D. A. Day, P. A. Cleary, P. J. Wooldridge, D. B. Millet, A. H. Goldstein, and R. C. Cohen (2007), The weekend effect within and downwind of Sacramento—Part 1: Observations of ozone, nitrogen oxides, and VOC reactivity, *Atmos. Chem. Phys.*, *7*(20), 5327–5339, doi:10.5194/acp-7-5327-2007.
Ng, N. L., J. H. Kroll, A. W. H. Chan, P. S. Chhabra, R. C. Flagan, and J. H. Seinfeld (2007), Secondary organic aerosol formation from *m*-xylene, toluene, and benzene, *Atmos. Chem. Phys.*, *7*(14), 3909–3922, doi:10.5194/acp-7-3909-2007.
Olivier, J. G. J., and J. J. M. Berdowski (2001), Global emission sources and sinks, in *The Climate System*, edited by J. Berdowski, R. Guicherit, and B. J. Heij, pp. 33–78, A.A. Balkema/Swets & Zeitlinger, Lisse, Netherlands.
Parrella, J. P., et al. (2012), Tropospheric bromine chemistry: Implications for present and pre-industrial ozone and mercury, *Atmos. Chem. Phys.*, *12*(15), 6723–6740, doi:10.5194/acp-12-6723-2012.
Parrish, D. D. (2006), Critical evaluation of US on-road vehicle emission inventories, *Atmos. Environ.*, *40*(13), 2288–2300, doi:10.1016/j.atmosenv.2005.11.033.
Paulot, F., J. D. Crounse, H. G. Kjaergaard, J. H. Kroll, J. H. Seinfeld, and P. O. Wennberg (2009a), Isoprene photooxidation: New insights into the production of acids and organic nitrates, *Atmos. Chem. Phys.*, *9*(4), 1479–1501, doi:10.5194/acp-9-1479-2009.
Paulot, F., J. D. Crounse, H. G. Kjaergaard, A. Kürten, J. M. St. Clair, J. H. Seinfeld, and P. O. Wennberg (2009b), Unexpected epoxide formation in the gas-phase photooxidation of isoprene, *Science*, *325*(5941), 730–733, doi:10.1126/science.1172910.
Pétron, G., et al. (2012), Hydrocarbon emissions characterization in the Colorado Front Range: A pilot study, *J. Geophys. Res.*, *117*, D04304, doi:10.1029/2011JD016360.

Pétron, G., et al. (2014), A new look at methane and non-methane hydrocarbon emissions from oil and natural gas operations in the Colorado Denver-Julesburg Basin, *J. Geophys. Res. Atmos.*, *119*, 6836–6852, doi:10.1002/2013JD021272.

Rodgers, C. D. (2000), *Inverse Methods for Atmospheric Sounding: Theory and Practice*, World Sci, Singapore.

Russell, A. R., L. C. Valin, and R. C. Cohen (2012), Trends in OMI $NO_2$ observations over the United States: Effects of emission control technology and the economic recession, *Atmos. Chem. Phys.*, *12*, 12,197–12,209, doi:10.5194/acp-12-12197-2012.

Sander, R. (1999), Compilation of Henry's law constants for inorganic and organic species of potential importance in environmental chemistry (Version 3). [Available at http://www.henrys-law.org.]

Schultz, M., L. Backman, Y. Balkanski, S. Bjoerndalsaeter, R. Brand, J. Burrows, S. Dalsoeren, M. de Vasconcelos, B. Grodtmann, and D. Hauglustaine (2007), REanalysis of the TROpospheric chemical composition over the past 40 years (RETRO)—A long-term global modeling study of tropospheric chemistry: Final report, Jülich/Hamburg, Germany.

Singh, H. B., L. J. Salas, B. K. Cantrell, and R. M. Redmond (1985), Distribution of aromatic hydrocarbons in the ambient air, *Atmos. Environ.*, *19*(11), 1911–1919, doi:10.1016/0004-6981(85)90017-4.

Singh, H. B., W. H. Brune, J. H. Crawford, D. J. Jacob, and P. B. Russell (2006), Overview of the summer 2004 Intercontinental Chemical Transport Experiment–North America (INTEX-A), *J. Geophys. Res.*, *111*, D24S01, doi:10.1029/2006JD007905.

Singh, H. B., W. H. Brune, J. H. Crawford, F. Flocke, and D. J. Jacob (2009), Chemistry and transport of pollution over the Gulf of Mexico and the Pacific: Spring 2006 INTEX-B campaign overview and first results, *Atmos. Chem. Phys.*, *9*(7), 2301–2318, doi:10.5194/acp-9-2301-2009.

Stein, O., M. G. Schultz, I. Bouarar, H. Clark, V. Huijnen, A. Gaudel, M. George, and C. Clerbaux (2014), On the wintertime low bias of Northern Hemisphere carbon monoxide found in global model simulations, *Atmos. Chem. Phys.*, *14*(17), 9295–9316, doi:10.5194/acp-14-9295-2014.

Toon, O. B., et al. (2010), Planning, implementation, and first results of the Tropical Composition, Cloud and Climate Coupling Experiment (TC4), *J. Geophys. Res.*, *115*, D00J04, doi:10.1029/2009JD013073.

van der Werf, G. R., J. T. Randerson, L. Giglio, G. J. Collatz, M. Mu, P. S. Kasibhatla, D. C. Morton, R. S. DeFries, Y. Jin, and T. T. van Leeuwen (2010), Global fire emissions and the contribution of deforestation, savanna, forest, agricultural, and peat fires (1997–2009), *Atmos. Chem. Phys.*, *10*(23), 11,707–11,735, doi:10.5194/acp-10-11707-2010.

Veres, P., J. B. Gilman, J. M. Roberts, W. C. Kuster, C. Warneke, I. R. Burling, and J. de Gouw (2010), Development and validation of a portable gas phase standard generation and calibration system for volatile organic compounds, *Atmos. Meas. Tech.*, *3*(3), 683–691, doi:10.5194/amt-3-683-2010.

Warneke, C., C. van der Veen, S. Luxembourg, J. A. de Gouw, and A. Kok (2001), Measurements of benzene and toluene in ambient air using proton-transfer-reaction mass spectrometry: Calibration, humidity dependence, and field intercomparison, *Int. J. Mass Spectrom.*, *207*(3), 167–182.

Warneke, C., et al. (2007), Determination of urban volatile organic compound emission ratios and comparison with an emissions database, *J. Geophys. Res.*, *112*, D10S47, doi:10.1029/2006JD007930.

Warneke, C., J. A. de Gouw, J. S. Holloway, J. Peischl, T. B. Ryerson, E. Atlas, D. Blake, M. Trainer, and D. D. Parrish (2012), Multiyear trends in volatile organic compounds in Los Angeles, California: Five decades of decreasing emissions, *J. Geophys. Res.*, *117*, D00V17, doi:10.1029/2012JD017899.

Wells, K. C., et al. (2012), Tropospheric methanol observations from space: retrieval evaluation and constraints on the seasonality of biogenic emissions, *Atmos. Chem. Phys.*, *12*(2), 3941–3982, doi:10.5194/acpd-12-3941-2012.

Wesely, M. L. (1989), Parameterization of surface resistances to gaseous dry deposition in regional-scale numerical models, *Atmos. Environ.*, *23*(6), 1293–1304.

White, M. L., et al. (2009), Are biogenic emissions a significant source of summertime atmospheric toluene in the rural Northeastern United States?, *Atmos. Chem. Phys.*, *9*(1), 81–92, doi:10.5194/acp-9-81-2009.

Xue, L. K., et al. (2014), Ground-level ozone in four Chinese cities: Precursors, regional transport and heterogeneous processes, *Atmos. Chem. Phys.*, *14*(23), 13,175–13,188, doi:10.5194/acp-14-13175-2014.

Yarwood, G., S. Rao, M. Yocke, and G. Whitten (2005), Updates to the carbon bond chemical mechanism: CB05, *Final report to the US EPA, RT-0400675*, *8*.

Zhang, Q., et al. (2009), Asian emissions in 2006 for the NASA INTEX-B mission, *Atmos. Chem. Phys.*, *9*(14), 5131–5153, doi:10.5194/acp-9-5131-2009.

Zhang, X., X. Lee, T. Griffis, A. Andrews, J. Baker, M. Erickson, N. Hu, and W. Xiao (2014a), Quantifying nitrous oxide fluxes on multiple spatial scales in the Upper Midwest, USA, *Int. J. Biometeorol.*, doi:10.1007/s00484-014-0842-4.

Zhang, X., X. Lee, T. J. Griffis, J. M. Baker, M. D. Erickson, N. Hu, and W. Xiao (2014b), The influence of plants on atmospheric methane in an agriculture-dominated landscape, *Int. J. Biometeorol.*, *58*, 819–833, doi:10.1007/s00484-013-0662-y.

Zhang, X., X. Lee, T. J. Griffis, J. M. Baker, and W. Xiao (2014c), Estimating regional greenhouse gas fluxes: An uncertainty analysis of planetary boundary layer techniques and bottom-up inventories, *Atmos. Chem. Phys.*, *14*(10), 10,705–10,719, doi:10.5194/acp-14-10705-2014.